IEEE Access
Multidisciplinary | Rapid Review | Open Access Journal

Received February 14, 2022, accepted March 3, 2022, date of publication March 8, 2022, date of current version March 16, 2022.

Digital Object Identifier 10.1109/ACCESS.2022.3157607

Jamming Effects on Hybrid Multistatic Radar Network Range and Velocity Estimation Errors

DILAN DHULASHIA, (Graduate Student Member, IEEE), MURAT TEMIZ, (Member, IEEE), AND MATTHEW A. RITCHIE, (Senior Member, IEEE)

Department of Electronic and Electrical Engineering, University College London (UCL), London WC1E 7JE, U.K.

Corresponding author: Dilan Dhulashia (dilan.dhulashia.15@ucl.ac.uk)

This work was supported in part by the Engineering and Physical Sciences Research Council (EPSRC) under Grant EP/R513143/1 and Thales U.K., in part by the University Defense Research Collaboration (UDRC), and in part jointly by the EPSRC and the Defense Science and Technology Laboratory (DSTL).

ABSTRACT This research studies the effects of three noise jamming techniques on the performance of a hybrid multistatic radar network in a selection of different electronic warfare (EW) situations. The performance metrics investigated are the range and velocity estimation errors found using the Cramér-Rao lower bounds (CRLBs). The hybrid multistatic network simulated is comprised of a single active radar transmitter, three illuminators of opportunity (IO), a receiver co-located at the active transmitter site, and two separately located silent receivers. Each IO transmits at a unique frequency band commonly used for civilian applications, including Digital Video Broadcasting-Terrestrial (DVB-T), Digital Audio Broadcasting (DAB), and FM radio. Each receiver is capable of receiving signals at all three IO frequency bands as well as the operating frequency band of the active radar transmitter. The investigations included compare the performance of the network at detecting a single airborne target under conditions where different combinations of jammer type, operating mode, directivity, and number of operating jammers are used. The performance degradation of the system compared to operation in a non-contested environment is determined and a comparison between the performance of the hybrid multistatic radar with that achievable by a monostatic radar and an active-only multistatic radar network within a selection of contested scenarios is made. Results show that the use of spatially distributed nodes and frequency diversity within the system enable greater theoretical functionality in the presence of jamming over conventional radar systems.

INDEX TERMS Cramér-Rao lower bounds, hybrid radar, multistatic radar, radar jamming.

I. INTRODUCTION

Multistatic hybrid radar networks combine the use of multiple transmitter and receiver nodes within a spatially distributed system capable of operating in both active and passive modes in a cooperative way. Such systems offer greater area coverage, multiple observation perspectives, frequency diversity and simultaneous multi-role functionality. They are of particular interest within military contexts as they offer a number of key advantages over conventional systems, including graceful degradation, covertness due to silent receivers located separately from active transmitters and the capability to perform passive sensing using signals from illuminators of opportunity (IO), thereby creating a radar system which is more resilient to adversarial jamming while maintaining the ability to use nodes in a monostatic configuration when necessary [1]. Multiple perspective detection can offer greater robustness and superior performance compared to single perspective systems by allowing for the facilitation of fused decision making based on data collected from multiple nodes. The increased complexity of a hybrid multistatic radar system allows both active and passive nodes to function with varying operating characteristics and for different nodes to simultaneously perform different roles. In order to effectively benefit from the additional functionality of such a system, informed decision making regarding the node distribution geometry, individual node task allocation, and optimal operating characteristics for a given role within a given scenario is of crucial importance. The efficacy with which this can be done depends on the availability of performance measure comparisons between different node pairs. An example of a vignette including a hybrid multistatic radar network operating within

The associate editor coordinating the review of this manuscript and approving it for publication was Fabrizio Santi.

an environment with multiple jamming modalities present and an airborne target can be seen in Fig. 1. This is representative of the nature of the types of scenarios which are modelled in this work.

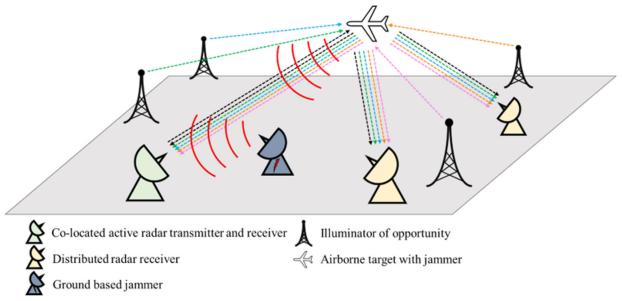

FIGURE 1. Illustrated vignette of hybrid multistatic radar network operating in a contested environment.

The ambiguity function (AF) and the Cramér-Rao lower bounds (CRLB) on radar measurement parameters are highly effective performance metrics. The AF is a method used to analytically determine the ability of a radar system to resolve two targets in range and velocity [2]. In monostatic configurations, the AF is based only on the transmitted waveform. A modified AF which additionally considers and accounts for the node geometry has been found in order to enable similar characterisation of bistatic configurations [3]. The CRLBs on range and velocity estimations in monostatic system configurations have been derived from the monostatic AF using the radar transmit waveforms. Derivations show that the CRLBs are found from the inverse of the Fisher information matrix (FIM), and a direct relationship between the AF and the FIM was shown in [4], thus enabling the CRLBs to be found from the AF. Previous work has shown that the CRLBs on range and velocity estimations can be similarly found for bistatic radar channels within multistatic systems by using the bistatic AF [5].

It has been shown that the bistatic CRLBs can be expressed in the form of a product which is separable into solely geometry dependent and waveform dependent parts. The FIM for Linear Frequency Modulated (LFM) [6], Sinusoidal Frequency Modulated (SFM) [7], and Orthogonal Frequency-Division Multiplexing (OFDM) [8] waveforms have been found and using these, the Root Cramér-Rao lower bounds (RCRLB) on range and velocity estimations were found and analysed for different multistatic scenarios in [9].

In [10], the CRLBs of target parameter estimations using a multistatic radar system under barrage jamming conditions were found and a method for finding an optimised solution to the directional power allocation of a jamming signal is proposed. The method aimed to maximise the CRLB metrics for target location and velocity using a particle swarm optimisation approach to find solutions to the non-convex problem and thereby achieve maximum network degradation. The model fidelity improved upon previous research by accounting for signal travel delay times and Doppler shifts due to target motion; however, the proposed method requires prior knowledge of the locations of receivers within the radar network such that the power allocations may be chosen. The locations of silent receivers may not always be known and is often highly dependent on the availability of situational information.

An algorithm based on the principles of using non-coherent integration detection is proposed in [11] with the aim of suppressing deception jamming and improving detection capabilities for a multistatic radar system. The method uses a discriminator to distinguish between jamming signals and true target returns at the centralised decision making level and is shown to improve system functionality. The vignette used in the work included multiple targets for simultaneous detection by a distributed radar network comprised of a single transmitter and seven receivers, including one receiver co-located with the transmitter node. The radar in this situation is then limited to using only an active radar waveform and single frequency band. A frequency diverse system capable of utilising multiple frequency bands would offer greater resilience to jamming methods, including deception jamming schemes, by requiring the jamming device to generate many jamming waveforms at a multitude of frequencies simultaneously. A frequency diverse multistatic system may then be able to outperform a system solely employing active radar waveforms, even with jamming suppression mechanisms in place, when operating in a contested electromagnetic (EM) environment. Alternatively, a frequency diverse multistatic system may be able to use such a suppression method with greater efficacy than an active radar based network, resulting in superior decision making capabilities.

Recent works have looked to implement methods based on providing convolutional neural networks with multistatic radar data such that jamming discrimination can be carried out using features beyond signal correlation [12]. The proposed method was shown to be effective against deception jamming techniques. The deception jamming problem is also addressed in [13], where the differences in the spatial scattering property between false and real targets is exploited as the basis of a method to differentiate between real targets and deception jamming. The complex modulation of signals from distributed receivers are correlated to facilitate a data fusion method based on local measurements without information loss as typically seen in centralised decision making employed by multistatic networks. However, the proposed approaches in [12] and [13] are only shown to be implemented on single frequency multistatic systems and do not leverage the capability of frequency diversity which such a platform may have the potential to support.

While interest in the use of passive systems continues to grow as a result of their ability to function without a dedicated active transmitter and their resilience to electronic countermeasures (ECM), the general limitations on the availability of research on the subject of ECM against passive radar systems within open literature is highlighted in [14] and [15]. It is

also suggested that deception jamming methods are of limited use against passive systems [16], demonstrating the need for systems with integrated passive capabilities but also validating the necessity for continued innovation to combat noise based jamming techniques, though the viability of deception jamming usage against networks involving passive pairs is disputed [17].

In [18], strategies for the jamming of Digital Audio Broadcasting (DAB) using noise based signals for the degradation of either the reference or the surveillance signal are proposed. In [19], a Gaussian noise waveform and a tone signal waveform were tested as jamming signals in simulations against a passive radar system utilising numerous civilian broadcasting waveforms as IOs, including Digital Video Broadcasting-Terrestrial (DVB-T), DAB, and FM radio. The reference channel and surveillance channel of the systems were targeted and the results showed that radar performance degradation can be reduced by using direct signal cancellation. The performance of an FM based passive coherent location (PCL) radar system under a selecion of jamming waveforms was studied in [20]. This work used a broadband noise jamming signal and a tone jamming signal at the carrier frequency to degrade the performance of the radar system. Results from simulations and experimental capture are compared under both jamming techniques. The authors show that the effectiveness of jamming against a passive radar system is dependent on the channel targeted and that FM jamming can be effective at relatively low jamming power. A study concentrating on the jamming of DVB-T based passive radar was carried out in [21] where it was shown how the deterministic content independent part of a DVB-T signal can be used as an effective ECM method. The authors highlight the importance for jamming to be directed to the surveillance channel of the radar system due to demodulation and remodulation protocols used in the reference channel which would render jamming targeting the reference channel ineffective. Techniques which can be exploited by the radar system to mitigate or reduce the jamming effects are also suggested; however, the effectiveness of electronic counter-countermeasures is likely to be inferior compared to being able to switch operation mode to use alternative IOs which are not being congested, thus making a system with multi-frequency capabilities desirable.

Finally, a method for countering imaging passive radar systems which use OFDM waveforms was proposed in [22]. The work describes an ECM technique which is utilised by a target based jammer for the purpose of protection against detection, localisation, and identification. The assumed target is a ship with the on-board jammer capable of omnidirectional jamming. The DVB-T signal is received by the jammer and modified to include the appropriate delay, radar cross-section (RCS) modulations, and Doppler shifts prior to re-transmission. While the proposed method is successful in carrying out jamming against a single receiver node passive radar, a multistatic system using spatially distributed receivers would recognise incoherencies between the jamming signal received at each node, making this jamming method ineffective.

In this work, a hybrid multistatic radar system capable of operating at multiple frequency bands simultaneously is considered, with the aim of determining the feasibility for optimal selection of transmitter-receiver (Tx-Rx) pairs to be carried out in order to minimise the range and velocity estimation errors using the CRLB as a performance metric. A vignette involving the detection of a single flying target is chosen to be used across a range of different contested EM environment situations created by the use of three different jamming techniques. The signal-to-noise-and-jamming-ratio (SNJR) for quartets consisting of either an active or passive transmitter, receiver, jammer, and target are constructed and the FIMs for the bistatic CRLBs using a selection of active and passive waveforms are provided. It should be noted that, in the analysis within this work, mention of performance improvement or degradation is an explicit reference to the reduction or increase in the CRLB values for a given parameter, respectively. Similarly, the best performance is considered to be that which results in the lowest CRLB value for a given parameter, while the worst performance is that resulting in the highest CRLB value. The novel contributions made by the research in this study include:

- The development of three jamming techniques, two of which enable jamming over a diverse frequency range and are capable of degradation against both active and passive radar operations, as well as documentation of their use by multiple jamming devices within a realistic situational vignette based on a hybrid multistatic radar network.
- Calculation of the bistatic CRLBs for range and velocity estimation errors under noise jamming conditions. These bounds allow for the performance comparison to be made between node pairs within a hybrid or active-only multistatic system operating in contested EM environments.
- A quantitative comparison of the theoretical best performance of a hybrid multistatic system against conventional multistatic and monostatic radar systems when functioning in a contested EM environment.

The rest of this paper is organised as follows: Section 2 presents the system model used; Section 3 introduces the bistatic AF and the FIMs of the different waveform types investigated, as well as the bistatic CRLBs for the range and velocity estimations; Section 4 describes the methodology used in the simulations and the jamming techniques employed; Section 5 presents the results obtained in each of the scenarios investigated as part of the research. Finally, Section 6 concludes the work.

II. MULTISTATIC HYBRID RADAR MODEL

The scenarios simulated in this research are based on a hybrid multistatic radar system which is comprised of multiple active and passive transmitters and multiple receivers operating within contested environments in which RF jamming systems

are deployed. For a scenario absent of any jammers containing a single target, n_T transmitters, and n_R receivers, the scene is then made up of $n_T n_R$ transmitter-receiver-target groups. When a scenario includes instances of jammers, the inclusion of a jammer node within the transmitter-receiver-target group can be determined dependent on the operating mode of the jammer. A depiction of the bistatic geometry between a transmitter-target-receiver group, along with a jammer capable of targeting the receiver within the group, is shown in Fig. 2.

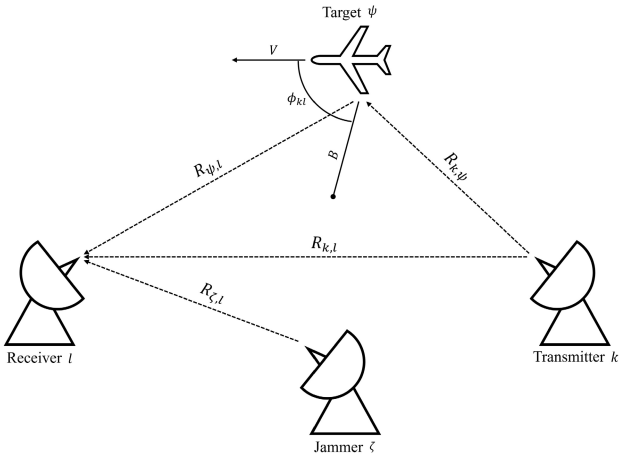

FIGURE 2. Bistatic geometry between transmitter, target and receiver group.

The distances between the nodes and target in the grouping are shown in Fig. 2. The distance between the kth transmitter and lth receiver is given by $R_{k,l}$, the distance between the kth transmitter and ψth target is $R_{k,\psi}$, and the distance between the ψth target and lth receiver is $R_{\psi,l}$. Finally, the distance from the ζth jammer to the lth receiver is denoted $R_{\zeta,l}$. The term ϕ_{kl} denotes the angle created between the velocity vector of the target ψ with the bistatic bisector B. The bistatic radial velocity of the target is then given by $V_{radial} = Vcos\phi_{kl}$, where V is the velocity of the target.

Based on the bistatic geometry between the transmitter-target-receiver triad forming a group excluding a jammer node, it is then possible to formulate expressions describing the instantaneous received signal at the lth receiver at time t due to a transmission signal originating from the kth transmitter which has been reflected from target ψ, given by $y_{l:k}(t)$. Such an expression is made up of the sum of terms relating to the direct path interference, the target response, and a noise term and is given by

$$\begin{aligned} y_{l:k}(t) = &\sqrt{\varphi_{kl}(t)\gamma_{kl}(t)}u(t-\tau_{kl}) \\ &+\sqrt{\varphi_{kl}(t)\sigma_{\psi}(t)\left[\gamma_{k\psi}(t)+\gamma_{\psi l}(t)\right]} \\ &\times u(t-\tau_{\psi})e^{-j2\pi\omega_{\psi}(t)}+n_l(t), \end{aligned} \tag{1}$$

where $\sigma_{\psi}(t)$, τ_{ψ}, and $\omega_{\psi}(t)$ are the target RCS at time t, delay caused by target range, and target Doppler frequency for target ψ, respectively. The term τ_{kl} denotes the delay in the reference channel formed between transmitter k and receiver l, and n_l is the additive white Gaussian noise (AWGN) at the lth receiver's surveillance antenna at time t. Finally, $\gamma_{ab}(t)$ denotes the instantaneous path loss between any RF source a and receiver b at time t and $\varphi_{ab}(t)$ is a term which encompasses the instantaneous power and gain characteristics for any pair of RF source a and receiver b given by

$$\varphi_{ab}(t) = P_a(t)G_a(t)G_b(t), \tag{2}$$

where $P_a(t)$ and $G_a(t)$ are the transmit power and gain of RF source a and $G_b(t)$ is the gain of receiver b at time t. It should be noted that the RF source here can be any transmitter, including active radar transmitters, IOs, and jammers.

Considering the quartet group of nodes, including a transmitter, target, receiver, and jammer, it is possible to formulate expressions for the SNJR for both an active radar and a passive radar case. In the active radar case, the SNJR at receiver l using an active radar transmitter k to detect a target ψ while being jammed by jammer ζ is approximated by

$$\rho_{l:k,\psi,\zeta} = \frac{\varphi_{kl}(t)\sigma_{\psi}(t)\left[\gamma_{k\psi}(t)+\gamma_{\psi l}(t)\right]}{k_B T_0 B_l N_{F_l}+\varphi_{\zeta l}(t)\gamma_{\zeta l}(t)}. \tag{3}$$

In the passive radar case, the SNJR at receiver l using an IO transmitter m to detect a target ψ while being jammed by jammer ζ is approximated by

$$\rho_{l:m,\psi,\zeta} = \frac{\varphi_{ml}(t)\sigma_{\psi}(t)\left[\gamma_{m\psi}(t)+\gamma_{\psi l}(t)\right]}{2k_B T_0 B_l N_{F_l}+\mu_{DPI}\varphi_{ml}\gamma_{ml}+\varphi_{\zeta l}(t)\gamma_{\zeta l}(t)}, \tag{4}$$

where μ_{DPI} is the residual direct-path interference (DPI) ratio which acts as a coefficient measuring the effectiveness of the DPI cancellation scheme used by the passive radar. In the simulations carried out in this research, a value for μ_{DPI} is chosen such that 50 dB of suppression is assumed for the direct path return. The target RCS and the path losses are chosen to be time independent and target RCS is also simplified to be aspect angle independent, meaning these two parameters may be treated as constants. It should also be noted that the path loss is a function of the wavelength and the distance traversed by the signal.

III. BISTATIC CRAMÉR-RAO LOWER BOUNDS ON RANGE AND VELOCITY ESTIMATIONS

The CRLBs provide a theoretical lower bound for the variance of an unbiased estimator for a deterministic parameter and are therefore a useful measure to obtain an optimised performance bound for the range and velocity estimation errors achievable, irrespective of processing technique limitations. The CRLBs can be obtained by taking the inverse of the FIM, for which a relationship to the AF has been derived [4]. It has been determined that the bistatic CRLBs reduce to those of the monostatic CRLBs when the radar geometry is such that the baseline between transmitter and receiver is zero.

The bistatic FIM is given by

$$J(R_{\psi l}, V_r) = -2\rho_{l:k,\psi,\zeta}\begin{bmatrix} \frac{\partial^2\Phi(R_{\psi,l}, V_r)}{\partial R_{\psi,l}^2} & \frac{\partial^2\Phi(R_{\psi,l}, V_r)}{\partial R_{\psi,l}\partial V_r} \\ \frac{\partial^2\Phi(R_{\psi,l}, V_r)}{\partial V_r\partial R_{\psi,l}} & \frac{\partial^2\Phi(R_{\psi,l}, V_r)}{\partial V_r^2} \end{bmatrix}, \quad (5)$$

where V_r denotes the radial velocity of the target along the bistatic bisector, $R_{\psi,l}$ is the range from the target ψ to the receiver l, $\rho_{l:k,\psi,\zeta}$ is the SNJR at receiver l using a transmitter k to detect a target ψ while being jammed by jammer ζ, and Φ is the square of the bistatic AF and is therefore given by

$$\Phi(\tau, \omega) = \left| \int_{-\infty}^{\infty} u(t)u^*(t-\tau)e^{-j2\pi\omega t}dt \right|^2, \quad (6)$$

where $u(t)$ is an arbitrary waveform and τ and ω are a time delay and a Doppler frequency for a bistatic geometry, as shown in [5], for which the AF (and therefore Φ) are being calculated.

The partial derivatives which make up the bistatic FIM are each separable into sums of products comprised of partial derivatives dependent only on geometric parameters and elements from the waveform exclusive FIMs. These waveform dependent FIMs have been derived for each of the waveforms used in this research in prior literature and are given along with mathematical descriptions of each of the waveforms used for the hybrid radar system in the following subsections, denoted by the type of modulation used to generate the waveform. The bistatic CRLBs for time delay τ (corresponding to range) and Doppler frequency ω (corresponding to velocity) are then given by

$$\text{CRLB}(\tau) = \frac{1}{2S_p\rho} \cdot \frac{J_{2,2}}{\det J}, \quad (7)$$

$$\text{CRLB}(\omega) = \frac{1}{2S_p\rho} \cdot \frac{J_{1,1}}{\det J}, \quad (8)$$

where J denotes the bistatic FIM, calculated based on the geometry and the waveform of the Tx-Rx pair and its detailed analytical derivations are given in [5]. Moreover, S_p indicates the integration gain due to utilising multiple LFM pulses or multiple DVB-T and DAB symbols, and ρ denotes the SNJR at the receiver.

In the following subsections, the signal models for each of the modulation schemes used by the four waveforms which can be used by the radar system are provided, as well as the FIMs for each scheme.

A. LINEAR FREQUENCY MODULATION (LFM)

The LFM waveform is a pulse compression commonly used by frequency-modulated continuous-wave (FMCW) radar systems and often described as a chirp waveform. The frequency of the signal is linearly increased over the chirp period. The LFM waveform at time t is given by

$$Y_{LFM}(t) = \begin{cases} Ae^{j\pi\frac{f_B}{T_C}t^2} & 0 \le t \le T_C \\ 0 & \text{other,} \end{cases} \quad (9)$$

where A is the amplitude of the chirp, f_B is the bandwidth of the chirp, and T_C is the chirp length. The quotient made up of the chirp bandwidth and chirp length is commonly referred to as the slope rate in radar waveform design.

Analytical expressions for the CRLB of an LFM waveform consisting of a sequence of chirps have previously been derived [6] and the FIM matrix for the range and Doppler measurements using the LFM waveform is

$$J_{LFM} = \begin{bmatrix} \frac{-\pi^2 f_B^2}{3} & \frac{\pi^2 f_B T_C}{3} \\ \frac{\pi^2 f_B T_C}{3} & \frac{\pi^2 T_{PRI}(1-N^2) - \pi^2 T_C^2}{3} \end{bmatrix}, \quad (10)$$

where N is the number of chirps in the LFM waveform and T_{PRI} is the pulse repetition interval.

B. SINUSOIDAL FREQUENCY MODULATED (SFM)

FM radio signals are an example of a commonly used SFM waveform and are used within the simulations included in this research. Their use in passive radar systems has been of growing interest due to the high powers used for transmission and a frequency band which is relatively low compared to those used by alternative potential IOs. Both of these characteristics result in a large area coverage being possible, as well as signal-to-noise-ratios (SNR) at typical radar ranges which make target sensing achievable.

An approximation of an FM radio signal made over an observation window must be made since the time variance of the frequency of the signal is dependent on the instantaneous signal content, meaning it is not possible for an exact model to be constructed. This approximation is given by

$$Y_{SFM}(t) = \begin{cases} \frac{A}{\sqrt{T_d}}e^{j\beta sin(2\pi f_0 t+\phi)} & 0 \le t \le T_d \\ 0 & \text{other,} \end{cases} \quad (11)$$

where A is the amplitude of the chirp, T_d is the observation duration, ϕ is the phase, and f_0 and β are terms arising when the bandwidth of the signal is approximated using Carson's bandwidth, given by

$$B_c = 2(\delta f + f_m) = 2\beta f_0, \quad (12)$$

where the peak frequency deviation and the highest frequency present in the modulating signal are given by δf and f_m, respectively.

The FIM and CRLB expressions must also be approximated for the FM signal since the characteristics of the waveform are also related to the instantaneous frequency which is a function of the signal content. Therefore, a modified expression for the FIM resulting from the approximated model in 11 is given by [7]

$$J_{SFM} = N\begin{bmatrix} 4\pi^2\beta^2 f_0^2 & -(-1)^{T_d f_0}2\pi\beta sin(\phi) \\ -(-1)^{T_d f_0}2\pi\beta sin(\phi) & \frac{\pi^2 T_d^2}{3} \end{bmatrix}. \quad (13)$$

C. ORTHOGONAL FREQUENCY-DIVISION MULTIPLEXING (OFDM)

OFDM is a multi-carrier waveform standard, of which each subcarrier is modulated with phase shift keying (PSK) or quadrature amplitude modulation schemes to entirely utilise the available channel and mitigate the impact of the multi-paths. OFDM waveforms are widely used in modern wireless communication and broadcasting systems, since OFDM modulation maximises the spectral efficiency of the communication channels by dividing wide band channels into narrow band multiple channels. OFDM signals are also considered for radar sensing to enable joint communication and radar functions [23]. The simulated scenarios carried out in this work incorporate two types of widely used digital broadcasting technologies: the DAB and DVB-T, which utilise OFDM signals. An OFDM signal can be expressed by

$$Y_{OFDM}(t) = \sum_{q=0}^{Q-1} \sum_{n=\frac{-N_s}{2}}^{\frac{N_s}{2}-1} A s_{n,q} e^{j2\pi n \Delta f (t - Tc - qT_Q)} w(t - qT_Q), \tag{14}$$

where N_S is the number of subcarriers, Q is the number of QAM symbols transmitted, $s_{n,q}$ denotes the qth QAM symbol transmitted in the nth subcarrier, A is the signal amplitude, Δf is the subcarrier frequency spacing, T_Q is the symbol duration, T_c is the cyclic-prefix duration, and $w(t)$ defines a root raised-cosine (RRC) filter response at t. A modified FIM for OFDM signals was derived in [8] and its elements are given by

$$[J_{OFDM}]_{1,1} = \frac{4\pi^2 Q(3 + \Delta f^2(N_s^2 - 1)(4T_Q - T_w)T_w)}{T_w(48T_Q - 12T_w)}, \tag{15}$$

$$[J_{OFDM}]_{2,2} = \frac{Q}{12T_Q - \frac{3}{4}T_w} \cdot \Big[4\pi^2 Q^2 T_Q^3 - \pi^2(Q^2 + 2)T_Q^2 T_w - (\pi^2 - 6)T_w^3 + 12(\pi^2 - 8)T_Q T_w^2\Big], \tag{16}$$

$$[J_{OFDM}]_{1,2} = [J_{OFDM}]_{2,1} = 0, \tag{17}$$

where T_w is the duration of the window of a raised cosine filter. The OFDM waveform parameters for the DVB-T and DAB signals are provided in Table 1. along with the numerical values of the parameters used for the LFM and FM signals used within the simulations in this work. The carrier frequency, f_c, is required for the calculation of the SNR and has therefore also been included within Table 1 for each waveform.

IV. METHODOLOGY

This section initially introduces the simulations which are carried out as part of the research before going on to describe the jamming techniques used within the investigations.

TABLE 1. Active and passive radar waveform parameters.

Waveform Type	Parameter-Value Pair
LFM	$f_c = 10$ GHz $f_B = 50$ MHz $T_C = 200\ \mu$s $T_{PRI} = 400\ \mu$s $N = 64$ $P_t = 5$ KW
FM	$f_c = 100$ MHz $f_0 = 15$ KHz $\beta = 5$ $T_d = 100$ ms $\phi = 0$ $P_t = 10$ KW
DVB-T	$f_c = 500$ MHz $\Delta f = 1116$ Hz $N_s = 6816$ $Q = 64$ $T_Q = 896\ \mu$s $T_w = T_Q/4$ $P_t = 7.5$ KW
DAB	$f_c = 150$ MHz $\Delta f = 2000$ Hz $N_s = 768$ $Q = 64$ $T_Q = 623\ \mu$s $T_w = T_Q/4$ $P_t = 5$ KW

A. SIMULATED SCENARIOS

A possible 1970 different scenario variations are possible based on the single selection of a node entity geometry and three jammers, each capable of transmitting in six possible jamming modes at two different directivities. In this work, a selection of 17 different scenarios are specifically chosen for study in order to provide the most meaningful results from scenarios most reflective of those which may be encountered in real world electronic warfare (EW) situations. The jamming modes and jammer selection of each of these scenarios are summarised in Table 2. It should be noted that J_{ground} and J_{target} are abbreviations for 'ground jammer' and 'target based jammer', respectively.

The hybrid multistatic radar network used in this research is made up of seven spatially distributed nodes, including four transmitters and three receivers. Each transmitter is capable of transmitting a unique waveform type, including LFM (active radar), DVB-T, FM, and DAB. One receiver is co-located with the transmitter capable of transmitting the LFM waveforms; however, all three receivers are capable of receiving all four waveforms at any given instance. The vignette is chosen such that a single flying target travelling along a linear trajectory in the xy-plane at constant altitude is considered in each of the 17 contested and one uncontested scenarios investigated. A map depicting the scenario used in the simulations in this work is shown in Fig. 3. This map shows the relative positions of the different nodes which comprise the hybrid multistatic radar system being used, as well as the locations of the two ground jamming nodes and the flight path of the target. It should be noted that in certain scenarios where a target based jammer is employed, the position of this jammer

TABLE 2. Jammer configurations used in each scenario simulated.

Scenario	No. J_{target}	No. J_{ground}	J_{target} mode	J_{ground} mode	J_{target} directivity	J_{ground} directivity
Clean	0	0	-	-	-	-
1	1	0	LFM	-	Directive	Directive
2	1	0	Random	-	Directive	Directive
3	1	0	Distance	-	Directive	Directive
4	0	2	-	LFM	Directive	Directive
5	0	2	-	Random	Directive	Directive
6	1	2	LFM	LFM	Directive	Directive
7	1	2	Random	Random	Directive	Directive
8	1	2	Distance	LFM	Directive	Directive
9	1	2	Distance	Random	Directive	Directive
10	1	2	LFM	Random	Directive	Directive
11	1	0	LFM	-	Omni	Omni
12	1	0	Random	-	Omni	Omni
13	1	0	Distance	-	Omni	Omni
14	0	2	-	LFM	Omni	Omni
15	0	2	-	Random	Omni	Omni
16	1	2	LFM	LFM	Omni	Omni
17	1	2	Random	Random	Omni	Omni

is equivalent to the position of the target at any given instance and thus follows the same flight path shown on the map. The locations of the nodes within the radar network, the two ground jammers within the environment, and the flight path of the target remain the same in all investigated scenarios. The precise coordinates of the positions for each entity, including the parametric equation for the position of the target at time t, are provided in Table 3. It should also be noted that, in all scenarios where the ground jammers are used, both jammers are transmitting the same waveforms.

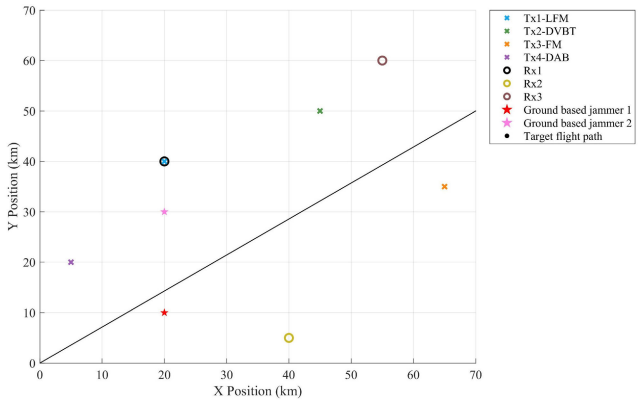

FIGURE 3. Map showing locations of transmitters, receivers, jammers, and target flight path, used in simulated scenario vignettes.

B. LFM JAMMING

This jamming method aims to only jam the active radar frequencies and to force the radar network to resort to utilising passive IOs. The technique assumes that the active radar frequency band is known. The jammer then continuously transmits a barrage style, zero mean, Gaussian jamming signal at the carrier frequency used by the active radar and which spans the bandwidth of the receiver channel dedicated to reception of the active radar waveform. The variance of the jamming signal is equal to the jamming signal power.

C. RANDOMISED JAMMING

This jamming technique uses a randomised selection method to choose the noise jamming waveform carrier frequency and bandwidth at each discrete instance within the simulation. The probability of the LFM (active radar) frequency band and characteristics being selected for jamming is given a biased weighting since this waveform is used to jam the active radar operation and is therefore the radar operation typically of greatest desirability to inhibit within a hybrid system from the perspective of the jammer. The probability for any of the three passive waveform characteristics being chosen for jamming is given by $P(Y_J(t) = Y_{passive}(t)) = \frac{1}{5}$, where $Y_{passive}$ can be a noise signal with characteristics determined be any of the DVB-T, DAB, or FM signal waveforms. The probability that the characteristics of the LFM waveform are chosen for the jamming waveform at any instancebre is $P(Y_J(t) = Y_{LFM}(t)) = \frac{2}{5}$.

D. DISTANCE JAMMING

This jamming technique selects the noise jamming waveform characteristics based on a determination of which transmitter within the scene is located at the shortest distance from the jammer at any given instance. The distance from the jammer to each transmitter is determined at each progressive time increment throughout the simulation and the jammer waveform is changed at the instance when the nearest transmitter changes. The jammer proceeds to transmit a jamming waveform with the characteristics corresponding to this transmitter until the instance when a different transmitter is determined to be at a proximity closer to the target. Thus, the index for the transmitter whose waveform characteristics are selected to be used for jamming at a given time instance is given by

$$K = \arg\min_{k} \left(R_{k,\psi}\right), \tag{18}$$

where $k = \{1, \ldots, n_T\}$ and, as before, $R_{k,\psi}$ denotes the range from transmitter k to target ψ. For the hybrid multistatic radar

simulated in this work $n_T = 4$. The label of the selected transmitter at the given time instance is then TxK.

The terms J0, J1, and J2 in Table 3 refer to the target based jammer, ground based jammer 1, and ground based jammer 2 from the map in Fig. 3, respectively. It should also be noted that the inclusion of two numerical values for the gain of each of the jammers is due to two directivities being possible. The larger number, quoted in decibels, refers to the jammer transmit gain when the jammer is used in the directive mode and is concentrating radiated energy towards a single receiver node. The smaller number, quoted in decibel isotropic, refers to the jammer transmit gain when the jammer is used in the omnidirectional mode and is radiating in all directions.

E. AVERAGE MINIMUM CRLB SELECTION ALGORITHM

The average minimum CRLB is the CRLB value demonstrative of the case where the multistatic radar system is capable of intelligently selecting the optimal pair at every instance. It is therefore the CRLB value for either range or velocity, obtained by averaging the CRLB value found at each time instance within the simulation runtime by the optimally performing Tx-Rx pair at each instance. This value then gives an accurate idealised representation of the overall hybrid multistatic network performance when operating within the contested environment conditions. The indexes of the optimally performing Tx-Rx pair at a discrete time instance t for a parameter ε which can be either range or velocity is given by

$$K_{\varepsilon:opt}(t), L_{\varepsilon:opt}(t) = \arg\min_{k,l}(\text{CRLB}_{\varepsilon:k,l}(t)), \tag{19}$$

where $\text{CRLB}_{\varepsilon:k,l}(t)$ denotes the CRLB value on parameter ε for the Tx-Rx pair formed by transmitter k and receiver l at time t. The possible transmitter index values are $k = \{1, \ldots, n_T\}$ and receiver index values are $l = \{1, \ldots, n_R\}$.

The average minimum CRLB for parameter ε across the simulation runtime is then given by

$$\text{CRLB}_{avg.min.\varepsilon} = \frac{1}{N_D}\sum_{t=1}^{N_D}\text{CRLB}_{\varepsilon:K_{\varepsilon:opt}(t),L_{\varepsilon:opt}(t)}(t), \tag{20}$$

where N_D is the total number of discrete time instances within a simulation runtime and $\text{CRLB}_{\varepsilon:K_{\varepsilon:opt}(t),L_{\varepsilon:opt}(t)}(t)$ is the CRLB value for parameter ε at time t due to the optimal Tx-Rx node pair for parameter ε at time t, given by $K_{\varepsilon:opt}(t)$ and $L_{\varepsilon:opt}(t)$, respectively.

V. RESULTS

The results section of this paper is broadly split into four parts. Initially, examples of the effects of the three different jamming techniques are shown by study of a selection of the scenarios used within the research. Secondly, the average RCRLB for range and velocity estimations across the entirety of each simulation for each Tx-Rx pair are presented for every scenario investigated. Thirdly, the average minimum RCRLB degradation for range and velocity estimations for each scenario are presented. Finally, the theoretical improvements achievable in RCRLB for both range and velocity by the hybrid multistatic radar network over a monostatic radar (Tx1-Rx1 pairing) and an active-only multistatic radar (Tx1 paired with any receiver) are shown.

Examples of the variation in the RCRLB for range and velocity for each transmitter and receiver pair throughout the scenario simulation are provided here. The examples cover four of the scenarios investigated, including jamming free (clean), omnidirectional *LFM Jamming*, omnidirectional *Randomised Jamming*, and omnidirectional *Distance Jamming*, which appear in Table 2 as scenarios: clean, 11, 12, and 13, respectively. The purpose of these examples is to illustrate the effects of each jamming technique on the RCRLBs.

Figs. 4 and 5 show the RCRLB on range and velocity for each target position within the scenario where no jamming occurs. It should be understood that the sharp peaks in the RCRLB on both range and velocity observed in some of the plots occurs at points where a forward scatter geometry is formed between a Tx-Rx pair and the target.

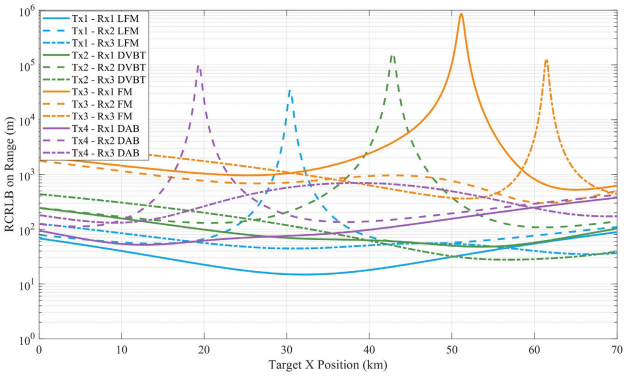

FIGURE 4. RCRLB on range at each target position in the clean scenario.

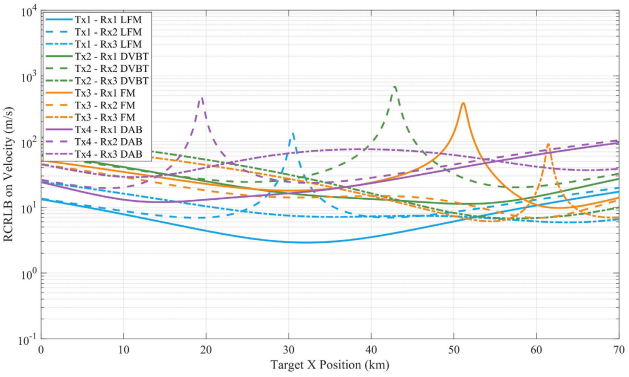

FIGURE 5. RCRLB on velocity at each target position in the clean scenario.

Figs. 6 and 7 show the RCRLB on range and velocity for each target position within the scenario where a single omnidirectional jammer located on the aircraft target is used and the jammer is transmitting the *LFM Jamming* technique

TABLE 3. Descriptions of function, operating characteristics, and position for each node in simulated vignette.

Node	Function	Power (W)	Gain	Waveform Type	Position (x,y,z) coordinates (m)
Tx1	Monostatic transmitter	5000	30 dB	LFM	(20k, 40k, 5)
Tx2	IO transmitter	7500	6 dB	DVB-T	(45k, 50k, 100)
Tx3	IO transmitter	10,000	2.15 dB	FM	(65k, 35k, 100)
Tx4	IO transmitter	5000	2.15 dB	DAB	(5k, 20k, 100)
Rx1	Monostatic receiver	-	2.15 dB	All	(20k, 40k, 2)
Rx2	Bistatic receiver	-	2.15 dB	All	(40k, 5k, 2)
Rx3	Bistatic receiver	-	2.15 dB	All	(55k, 60k, 2)
Target	Aircraft target	-	-	-	$(100t, \frac{500}{7}t, 400)$
J0	Target mounted jammer	10,000	20 dB or 5 dBi	All	On target
J1	Ground based jammer	25,000	20 dB or 5 dBi	All	(20k, 10k, 5)
J2	Ground based jammer	25,000	20 dB or 5 dBi	All	(20k, 30k, 5)

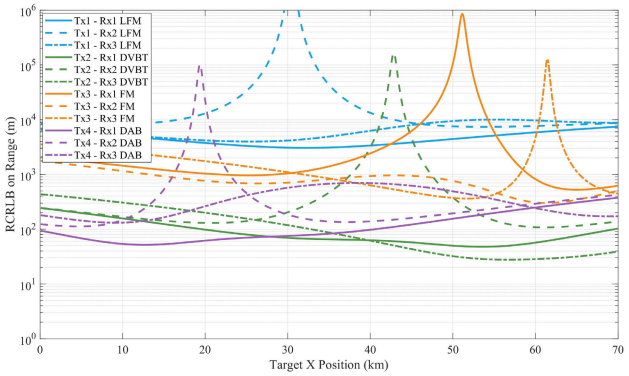

FIGURE 6. RCRLB on range at each target position in the LFM jamming scenario.

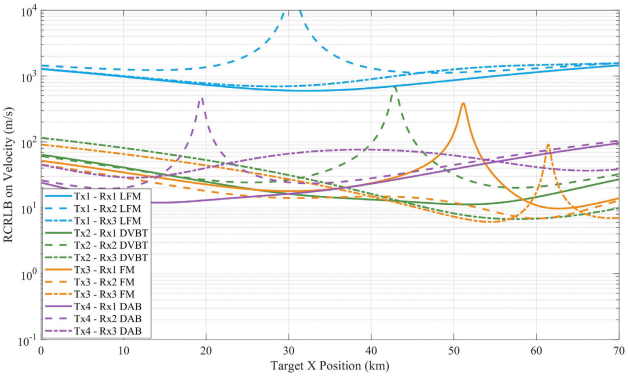

FIGURE 7. RCRLB on velocity at each target position in the LFM jamming scenario.

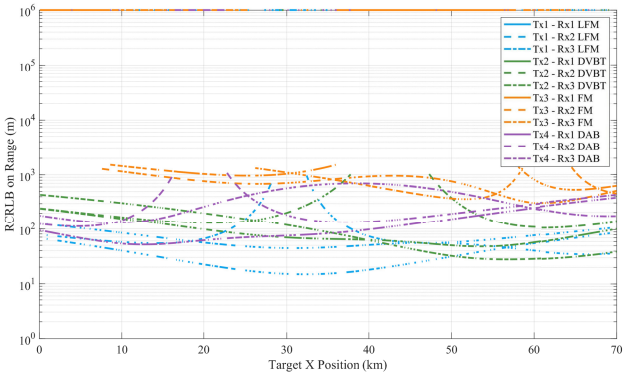

FIGURE 8. RCRLB on range at each target position in the random jamming scenario.

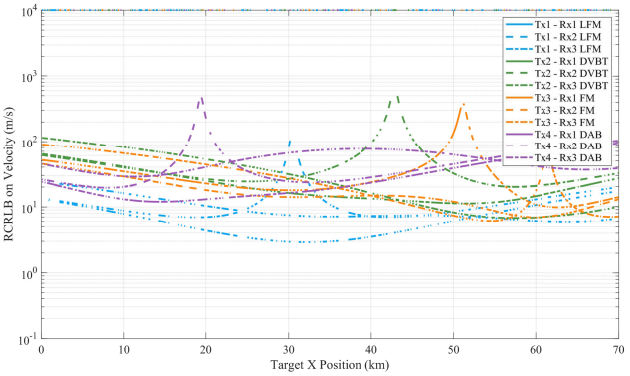

FIGURE 9. RCRLB on velocity at each target position in the random jamming scenario.

throughout the scenario. It can be determined from a comparison between Figs. 6 and 7 with Figs. 4 and 5, respectively, that the employment of this jamming technique results in severe degradation of the Tx1-Rx1 pair (monostatic) and the Tx1-Rx2 and Tx1-Rx3 pairs (active bistatic) performance for both the RCRLB on range and velocity. The performance of the node pairings which are operating passively are unaffected and generally outperform the active radar under the contested conditions. As such, under these jamming conditions, a strategic choice to select passive operation over active operation should be made. This evaluation can be made by comparison of the average RCRLB of each pair for the parameter of interest.

Figs. 8 and 9 show the RCRLB on range and velocity for each target position within the scenario where a single omnidirectional jammer located on the aircraft target performing the *Randomised Jamming* technique is used. It can be seen from the two figures that determination of the optimal Tx-Rx pair to use at any given instance becomes very difficult due to the sporadic nature of each plot and the often large deviations in RCRLB at neighbouring instances, making this an effective form of jamming for the purpose of reducing

the radar networks ability to choose node pairs based on average CRLBs. It should be noted that the plotted lines within Figs. 8 and 9 are shown to be discontinuous in order to aid visualisation by reducing the overlap between the lines belonging to different Tx-Rx pairs.

Figs. 10 and 11 show the RCRLB on range and velocity for each target position within the scenario where a single omnidirectional jammer located on the aircraft target performing the *Distance Jamming* technique is used. As can be seen from both figures, when the jamming waveform used is switched, the RCRLBs for the three plots pertaining to the corresponding transmitter/waveform become significantly degraded. This appears to form notches in the plots occurring at target positions for which a given transmitter is located closest to the target. A comparison between Figs. 10 and 11 with Figs. 4 and 5, respectively, shows that this jamming technique has resulted in points within the scenario where the node selection for optimal performance deviates from the selections which would be made when operating within the clean scenario. As such, this jamming technique would force the radar system to make intelligent choices regarding node pair selection and degenerates the optimum performance possible within particular time ranges within the scenario.

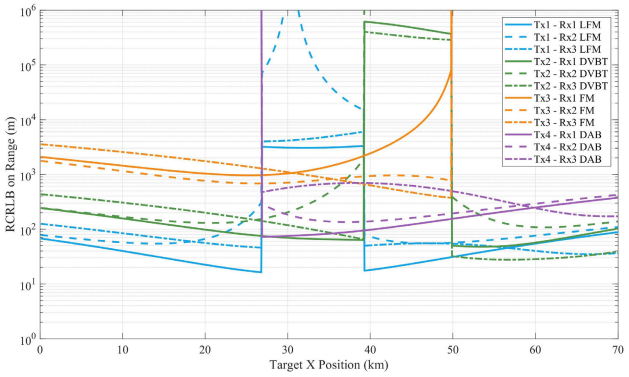

FIGURE 10. RCRLB on range at each target position in the distance based jamming scenario.

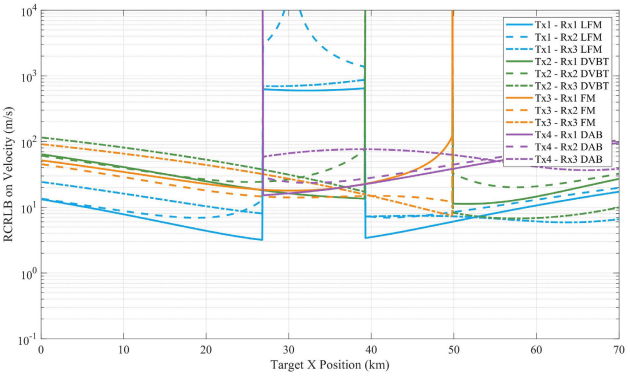

FIGURE 11. RCRLB on velocity at each target position in the distance based jamming scenario.

The results showing the average RCRLB on range and velocity for each waveform across all scenarios have been split into four separate graphs. The graphs in Figs. 12 and 13 correspond to the results from scenarios involving directive jamming for range and velocity, respectively, while those in Figs. 14 and 15 correspond to the results from scenarios involving omnidirectional jamming for range and velocity, respectively.

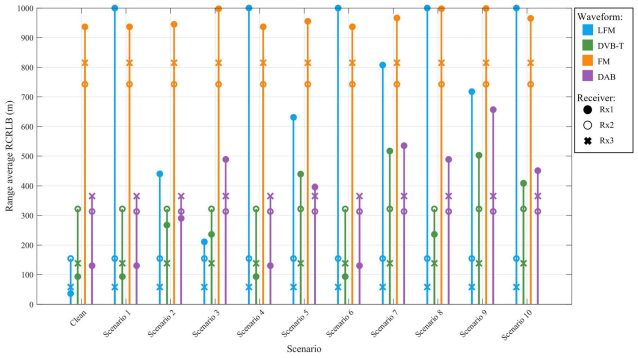

FIGURE 12. RCRLB on range at each receiver for each waveform mode for all scenarios with directive jamming.

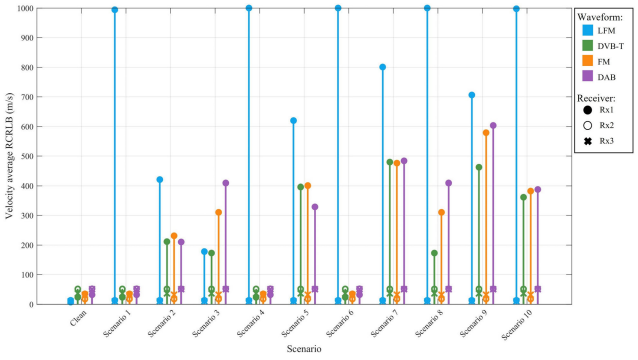

FIGURE 13. RCRLB on velocity at each receiver for each waveform mode for all scenarios with directive jamming.

As expected, it can be seen in Figs. 12 and 13 that no differences are observed in the results corresponding to Rx2 and Rx3 for all scenarios. This is due to the directivity of the jammers causing radiated energy to be concentrated towards Rx1 throughout the scenarios. In the 'Clean' scenario, the active radar transmitter (Tx1) with co-located receiver (Rx1) produces the best result, as would be expected since this is the pair forming a monostatic radar. The second highest performance is achieved using the active radar transmitter (Tx1) paired with Rx3 (a bistatic active radar). Since Rx3 is not affected by the directive jamming used in these scenarios, the Tx1-Rx3 pairing is also seen to perform the best in all the scenarios where jamming is used. Therefore, the further comments included here in reference to Figs. 12 and 13 refer only to the results concentrating on pairs involving Rx1 as the receiver node.

It can be seen from Fig. 12 that in all instances where the *LFM Jamming* technique is used by either the target based jammer or the ground jammers, the Tx1-Rx1 (LFM) pairing performance is severely degraded. When this method of jamming is used, the Tx2 (DVB-T) transmitter paired with Rx1 tends to perform the best in all scenarios, apart from Scenario 5. Where the *Randomised Jamming* method is employed, the Tx1-Rx1 (LFM) pair is degraded the most; however, Tx2-Rx1 (DVB-T) and Tx4-Rx1 (DAB) performances are also degraded. This jamming method is effective as it forces the radar system to use passive pairs by severely degrading the Tx1-Rx1 (LFM) pair; however, it also degrades the passive performance, albeit to a lesser extent. The *Distance Jamming* method had the greatest effect on the DAB waveform performance, though this is partially likely due to this waveform being targeted for jamming for the longest duration period during the simulated scenarios within which this jamming technique is used. The Tx3-Rx1 (FM) tends to perform poorly in all cases and only ever outperforms the LFM waveform. This occurs in five out of the ten scenarios and only where at least one jammer is utilising the *LFM Jamming* method. In scenarios involving either the *Randomised Jamming* or Distance Jamming, the pairings between IO transmitters and receivers located away from the active radar site outperform the pairings between the IO transmitters and Rx1. This shows the benefit of having a radar network inclusive of receivers located separately from transmitter nodes.

The Tx3 (FM) transmitter with Rx1 pairing performs more competitively with regards to RCRLB for velocity, as can be seen from Fig. 13, with values typically close to those achieved by Tx2-Rx1 (DVB-T) and Tx4-Tx1 (DAB). In nine out of the ten scenarios where jamming is used, the monostatic active radar result is degraded to a point where performance would be severely inferior to any of the other waveforms and receiver node choices. When considering the results of pairs involving Rx1, it can be seen that for seven out of the ten scenarios involving jamming, the DVB-T waveform performs at least marginally better than DAB and FM. In the three instances where this is not the case, the jamming technique used was the *Randomised Jamming* and therefore the degradation differences between the three passive waveforms would see some variation over a repetition of simulations and a performance ranking could be subject to change. In all scenarios, the degradation effect is such that the bistatic mode when operating with Tx1 (LFM) is superior to using Tx1 (LFM) in a monostatic configuration for both range and velocity average RCRLBs.

It should be noted that average range RCRLB values greater than 1000 m or average velocity RCRLB values greater than 1000 m s^{-1} were deemed to have been degraded beyond a point of further interest and as such are simply treated as being equal to a maximum possible value of 1000 in both cases.

From the results shown in Figs. 14 and 15, it can be seen that when the jammers operate omnidirectionally, the

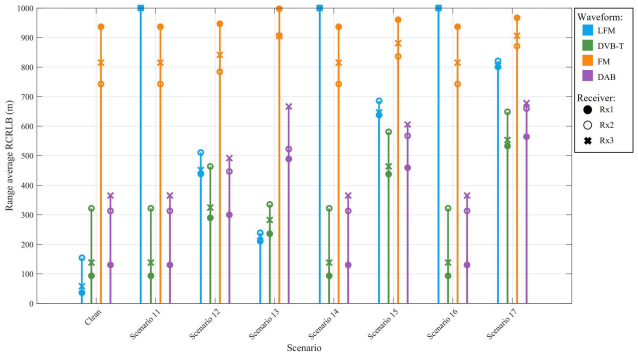

FIGURE 14. RCRLB on range at each receiver for each waveform mode for all scenarios with omnidirectional jamming.

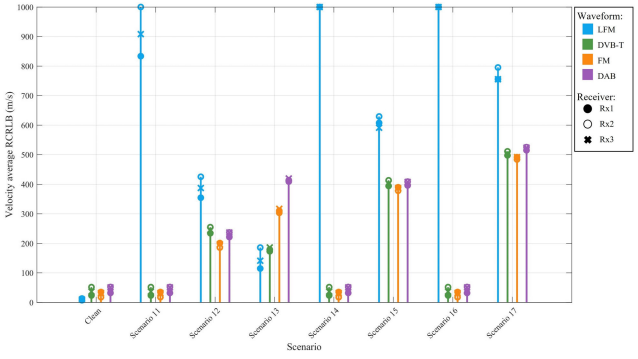

FIGURE 15. RCRLB on velocity at each receiver for each waveform mode for all scenarios with omnidirectional jamming.

performance of pairings involving all three receivers are degraded. In scenarios where the *LFM Jamming* technique is used, all receivers paired with Tx1 (LFM) are severely degraded regardless of whether they are in a monostatic or bistatic arrangement. However, the radar is still capable of using pairings involving Tx2 (DVB-T) and Tx3 (DAB) transmitters to reduce the degradation effect. This demonstrates the desirability for a multistatic radar network to be capable of utilising a range of frequency bands in order to maintain resilience to particular jamming methods. This also shows how jamming techniques which are diverse in frequency are better suited to disrupting hybrid multistatic radar operations compared to single frequency band jammers.

The scenarios involving the use of the *Distance Jamming* method again show that the pairs involving the Tx4 (DAB) transmitter are more degraded than those using other waveforms. This further shows the dependency of this jamming method's performance on node location. A modified version of the technique could look to utilise the information shown here to improve the technique's all-round performance by weighting the significance of each transmitter prior to decision making. This would result in a reduction of the radius around the Tx3 (FM) transmitter and increases in the radii around the Tx1 (LFM) and Tx4 (DAB) transmitters within which decisions are made to jam those waveform frequency ranges.

The average minimum RCRLB degradation for range and velocity for each scenario is shown in Figs. 16 and 17, respectively. The bars in the graphs of Figs. 16 and 17 show the performance degradation achieved by the jammers in each scenario relative to the results obtained in the 'clean' scenario, that is, the increase in RCRLB value between each scenario compared to the 'clean' scenario.

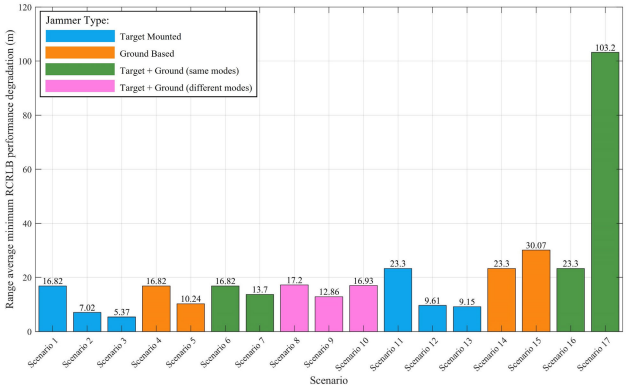

FIGURE 16. Minimum range RCRLB degradation from clean for all scenarios.

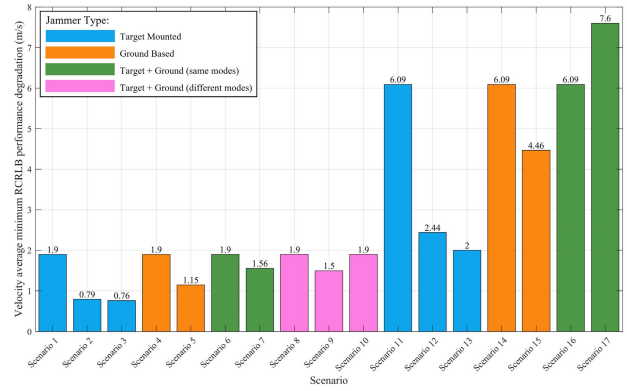

FIGURE 17. Minimum velocity RCRLB degradation from clean for all scenarios.

From Fig. 16, it can be determined that in scenarios where the jamming is directive, regardless of whether the target based jammer, ground based jammers, or a combination of both jamming modalities are used, the *LFM Jamming* technique is more effective than the *Randomised Jamming* technique or the *Distance Jamming* method (where data is available). In scenarios where the jamming is omnidirectional, it is seen that the most effective jamming method is dependent on the jamming modality. If a target based jammer is employed, the *LFM Jamming* technique achieves the highest performance degradation, while the *Randomised Jamming* method is most effective if only ground based jammers or ground based and a target based jammer are used in conjunction. In Fig. 16, it is also observed that when the jamming is directional, there is a small increase in performance degradation when using the mixed jamming arrangement such that the target based jammer utilises the *Distance Jamming* technique while the ground based jammers utilise the *LFM Jamming* technique. This configuration outperforms having all three jammers using the *LFM Jamming* technique by an additional degradation of 0.38 m.

Figs. 17 shows that the *LFM Jamming* technique is also seen to outperform the *Randomised Jamming* and *Distance Jamming* techniques at degrading the average minimum RCRLB on velocity when the jamming modality is a target based jammer or ground based jammers for both directive and omnidirectional jamming. When a combination of target based jammer and ground based jammers are used, it is seen that the *LFM Jamming* technique is most effective if the jamming is directive; however, when the jamming is omnidirectional the *Randomised Jamming* technique causes the greatest performance degradation. In the results from Fig. 17 no additional degradation is observed from using a combination of different jamming techniques from the two different jamming platform types.

The *Distance Jamming* method is seen to be the least effective method of jamming against the multistatic radar network for both the minimum average RCRLB on range and velocity, while the most effective jamming method when either a target based jammer or ground based jammers are used in isolation is typically the *LFM Jamming* technique for both range and velocity. However, it is seen that the overall most effective strategy for degrading the network performance on range estimations in the vignette chosen is to use a target based jammer alongside ground based jammers where all jammers are utilising the *Randomised Jamming* technique for both range and velocity estimates. This shows that greater jamming effectiveness can be achieved against a hybrid multistatic radar network by targeting all active and passive waveforms which the network is capable of utilising instead of solely attempting to degrade the active components.

Figs. 18 and 19 show the RCRLB improvements for range and velocity, respectively, when using the hybrid multistatic radar network capable of intelligent pair selection compared to the theoretical best performance values obtainable by the Tx1-Rx1 pair (monostatic radar) and the lowest value obtainable by either Tx1-Rx1, Tx1-Rx2 or Tx1-Rx3 (active-only multistatic radar) for each scenario involving omnidirectional jamming investigated. Intelligent pair selection for the hybrid multistatic system assumes, similarly to the analysis in Figs. 16 and 17, the average minimum RCRLB as the performance of the system.

The scenarios involving omnidirectional jamming (scenarios 11-17) were selected here, since the most significant performance improvements over an active-only multistatic system are achieved by a hybrid multistatic system when the jamming used against the systems is omnidirectional. Significant performance increases are seen for both directional and omnidirectional jamming when comparing a hybrid multistatic system with a monostatic system and small improvements are seen to be offered by the hybrid system over an active-only multistatic system in cases where

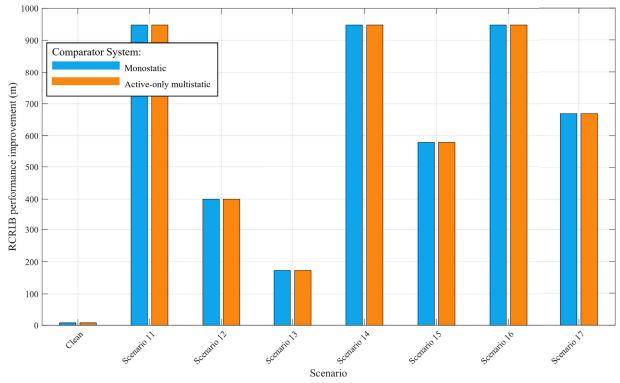

FIGURE 18. Improvement of estimation error on range using the average minimum RCRLB achieved by the hybrid multistatic radar network over a monostatic and an active-only multistatic radar network.

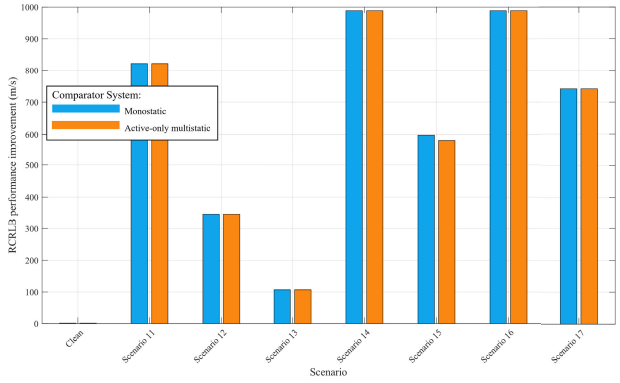

FIGURE 19. Improvement of estimation error on velocity using the average minimum RCRLB achieved by the hybrid multistatic radar network over a monostatic and an active-only multistatic radar network.

directional jamming is used. This is expected as two out of the three receiver nodes within the active-only multistatic system do not receive any jamming when directional jamming is used. It can be seen from Figs. 18 and 19 that the hybrid mulistatic system theoretically offers a potential performance advantage in every omnidirectional jamming based scenario tested and in the 'clean' scenario.

In scenarios where omnidirectional jamming is used, it can be seen that the RCRLB improvement achieved by the hybrid multistatic system over both the active-only multistatic and the monostatic system is drastic. This shows that the hybrid multistatic radar network offers significantly superior performance over conventional radar systems when operating within contested environments due to the frequency diversity opportunities such a system possesses.

VI. CONCLUSION

In this work, the effects of three jamming techniques on the theoretical performance limits of a hybrid multistatic radar system have been investigated. A vignette of a system comprised of four transmitters, including one active radar transmitter and three IOs, and three receivers, including one receiver co-located with the active radar site, is studied under a variety of jamming conditions caused by a target based jammer and ground based jammers utilising three different jamming techniques. The degradation in radar performance caused by each jamming methodology relative to operation in an uncontested environment is determined using the RCRLB on range and velocity estimations. Further, a comparison of the theoretical best achievable performance of a monostatic, active-only multistatic and hybrid multistatic radar is made for a selection of different jamming conditions. The results have shown that the average minimum RCRLB on range and velocity would be severely degraded for a multistatic radar system without the capability of frequency diversity and validate the desirability for a hybrid multistatic radar network to be capable of utilising numerous IOs to reduce the degradation of jamming effects. It is thus shown how a hybrid multistatic radar system can offer benefits over traditional systems for minimising performance degradation in the presence of jamming.

ACKNOWLEDGMENT

The authors would like to thank Thales U.K., DSTL, EPSRC, and the UDRC for their support and funding for this research.

REFERENCES

[1] H. Griffiths, "Multistatic, MIMO and networked radar: The future of radar sensors?" presented at the 7th Eur. Radar Conf., 2010.
[2] M. Skolnik, *Introduction to Radar Systems*, 3rd ed. Columbus, OH, USA: McGraw-Hill, 2001.
[3] T. Tsao, M. Slamani, P. Varshney, D. Weiner, H. Schwarzlander, and S. Borek, "Ambiguity function for a bistatic radar," *IEEE Trans. Aerosp. Electron. Syst.*, vol. 33, no. 3, pp. 1041–1051, Jul. 1997, doi: 10.1109/7.599331.
[4] H. L. Van Trees, *Detection, Estimation and Modulation Theory*, vol. 3. Hoboken, NJ, USA: Wiley, 1971.
[5] M. S. Greco, P. Stinco, F. Gini, and A. Farina, "Cramér–Rao bounds and selection of bistatic channels for multistatic radar systems," *IEEE Trans. Aerosp. Electron. Syst.*, vol. 47, no. 4, pp. 2934–2948, Oct. 2011.
[6] A. Dogandzic and A. Nehorai, "Cramér–Rao bounds for estimating range, velocity, and direction with an active array," *IEEE Trans. Signal Process.*, vol. 49, no. 6, pp. 1122–1137, Jun. 2001.
[7] M. S. Greco, P. Stinco, F. Gini, A. Farina, and M. Rangaswamy, "Cramér–Rao bounds and TX-RX selection in a multistatic radar scenario," in *Proc. IEEE Radar Conf.*, May 2010, pp. 1371–1376.
[8] A. Filip and D. Shutin, "Cramér–Rao bounds for L-band digital aeronautical communication system type 1 based passive multiple-input multiple-output radar," *IET Radar, Sonar Navigat.*, vol. 10, no. 2, pp. 348–358, 2016.
[9] M. Temiz, M. Ritchie, and H. Griffiths, "Waveform selection for multi-band multistatic radar networks," *IET Radar, Sonar Navigat.*, to be published.
[10] G. Zheng, S. Na, T. Huang, and L. Wang, "A barrage jamming strategy based on CRB maximization against distributed MIMO radar," *Sensors*, vol. 19, no. 11, p. 2453, May 2019.
[11] S. Zhang, Y. Zhou, L. Zhang, Q. Zhang, and L. Du, "Target detection for multistatic radar in the presence of deception jamming," *IEEE Sensors J.*, vol. 21, no. 6, pp. 8130–8141, Mar. 2021, doi: 10.1109/JSEN.2021.3050008.
[12] J. Liu, M. Gong, M. Zhang, H. Li, and S. Zhao, "An anti-jamming method in multistatic radar system based on convolutional neural network," *IET Signal Process.*, to be published, doi: 10.1049/sil2.12085.
[13] S. Zhao, L. Zhang, Y. Zhou, N. Liu, and J. Liu, "Discrimination of active false targets in multistatic radar using spatial scattering properties," *IET Radar, Sonar Navigat.*, vol. 10, no. 5, pp. 817–826, Jun. 2016.
[14] M. Knioła, T. Rogala, and Z. Szczepaniak, "Counter-passive coherent locator (C-PCL)—A method of remote detection of passive radars for electronic warfare systems," *Electronics*, vol. 10, no. 14, p. 1625, 2021. [Online]. Available: https://doi.org/10.3390/electronics10141625

[15] M. Inggs, C. Tong, D. O'Hagan, U. Bonigert, U. Siegenthaler, C. Schupbach, and H. Pratisto, "Noise jamming of a FM band commensal radar," in *Proc. IEEE Radar Conf.*, Oct. 2015, pp. 493–498, doi: 10.1109/RadarConf.2015.7411933.
[16] A. G. Westra, "Radar versus stealth: Passive radar and the future of U.S. military power," Inst. Nat. Strategic Stud., Nat. Defense Univ., Washington, DC, USA, Tech. Rep. ADA515506, 2009.
[17] J. Schuerger and D. Garmatyuk, "Deception jamming modeling in radar sensor networks," in *Proc. IEEE Mil. Commun. Conf. (MILCOM)*, Nov. 2008, pp. 1–7, doi: 10.1109/MILCOM.2008.4753118.
[18] C. Schüpbach and U. Böniger, "Jamming of DAB-based passive radar systems," in *Proc. Eur. Radar Conf. (EuRAD)*, Oct. 2016, pp. 157–160.
[19] D. W. O'Hagan, S. Paine, and C. Schüpbach, "Overview of electronic attacks against passive radar," in *Proc. Int. Appl. Comput. Electromagn. Soc. Symp. (ACES)*, Apr. 2019, pp. 1–2.
[20] S. Paine, D. W. O'Hagan, M. Inggs, C. Schupbach, and U. Boniger, "Evaluating the performance of FM-based PCL radar in the presence of jamming," *IEEE Trans. Aerosp. Electron. Syst.*, vol. 55, no. 2, pp. 631–643, Apr. 2019, doi: 10.1109/TAES.2018.2858158.
[21] C. Schupbach, D. W. O'Hagan, and S. Paine, "Electronic attacks on DVB-T-based passive radar systems," in *Proc. IEEE Radar Conf. (RadarConf)*, Apr. 2018, pp. 0417–0422, doi: 10.1109/RADAR.2018.8378595.
[22] E. Giusti, M. Martorella, A. Capria, M. Conti, C. Moscardini, and F. Berizzi, "Electronic countermeasure for OFDM-based imaging passive radars," in *Proc. Int. Conf. Radar (RADAR)*, Aug. 2018, pp. 1–4, doi: 10.1109/RADAR.2018.8557316.
[23] C. Sturm and W. Wiesbeck, "Waveform design and signal processing aspects for fusion of wireless communications and radar sensing," *Proc. IEEE*, vol. 99, no. 7, pp. 1236–1259, Jul. 2011, doi: 10.1109/JPROC.2011.2131110.

DILAN DHULASHIA (Graduate Student Member, IEEE) received the M.Eng. degree in electronic engineering with a focus on nanotechnology from University College London (UCL), London, U.K., in 2019, where he is currently pursuing the Ph.D. degree in electrical engineering. His research interests include radar system modeling and analysis, studying contested EM environments, and micro-Doppler signature classification.

MURAT TEMIZ (Member, IEEE) received the M.Sc. degree in electrical and electronics engineering from the TOBB University of Economics and Technology, Ankara, Turkey, and the Ph.D. degree in electrical and electronic engineering from the University of Manchester, U.K., in 2020. He is currently working as a Research Fellow with University College London (UCL), London, U.K. His current research interests include massive MIMO communication systems, dual-functional radar and communication systems, multistatic radar networks, passive radar systems, and applications of machine learning techniques in communication and radar systems.

MATTHEW A. RITCHIE (Senior Member, IEEE) received the M.Sc. degree in physics from The University of Nottingham, in 2008, and the Eng.D. degree from University College London (UCL), London, U.K., in association with Thales U.K., in 2013.

He then worked as a Postdoctoral Research Associate focusing on machine learning applied to multistatic radar for micro-doppler classification. In 2017, he took a Senior Radar Scientist position at the Defense Science and Technology Laboratories (DSTL). He is currently a Lecturer at UCL within the Radar Sensing Group and focused on areas including multistatic radar, passive radar, micro-Doppler and multi-role RF sensor hardware. Currently, he is the Chair of the IEEE Aerospace and System Society (AESS) for the U.K. and Ireland, is a Subject Editor-in-Chief of the *IET Electronics Letters* Journal and the Head of the U.K. EMSIG Society. He was a recipient of the 2017 IET RSN Best Paper Award and the Bob Hill Award at the 2015 IEEE International Radar Conference.